Urinary metabolomic signatures associated with early adverse events during volumetric modulated arc therapy for prostate cancer: A secondary analysis of a public dataset

MAI FUKUSHI[1], YOTA TATARA[2], HIDEKI OBARA[3] and SATORU MONZEN[1,4]

[1]Department of Radiation Science, Hirosaki University Graduate School of Health Sciences, Hirosaki, Aomori 036-8564, Japan; [2]Department of Stress Response Science, Biomedical Research Center, Graduate School of Medicine, Hirosaki University, Hirosaki, Aomori 036-8562, Japan; [3]Department of Radiology, Hirosaki University Hospital, Hirosaki, Aomori 036-8563, Japan; [4]Research Center for Biomedical Sciences, Hirosaki University, Hirosaki Graduate School of Health Sciences, Hirosaki, Aomori 036-8564, Japan

Received September 22, 2025; Accepted March 2, 2026

DOI: 10.3892/mco.2026.2953

Abstract. Volumetric modulated arc therapy (VMAT) is an advanced radiotherapy technique for prostate cancer that improves dose conformity but is often accompanied by early urinary toxicities. Non-invasive biomarkers for predicting such adverse events remain limited. In the present study, a secondary analysis of a public urinary metabolomics dataset (MxP® Quant 500; 630 metabolites) from 11 patients treated with VMAT (76 Gy/38 fractions) was performed. Patients were grouped as patients with urinary toxicities (n=7; Grade 1) and those without (n=4). Patient-level Spearman's rank correlation coefficients (ρ) between the metabolite concentration and fraction number were calculated and summarized within each group. Overlaps in the top 60 positively correlated metabolites and bottom 60 negatively correlated metabolites across groups were identified and assessed using OmicsNet 2.0. Four metabolites [cholesteryl ester 20:4, taurodeoxycholic acid, triglyceride (TG) 18:0_32:2 and TG 18:3_34:1] were positively correlated in the toxicity group but negatively correlated in controls. Conversely, five metabolites, including phosphatidylcholines (PCs; PC aa C42:2 and PC ae C42:1), TG 16:0_38:1, fatty acid (FA) 20:2 and diglyceride 18:1_18:1, showed the opposite trend. Network analysis indicated impaired lipolysis, specifically the hydrolysis of TGs into FAs, involving carboxyl ester lipase and adipose TG lipase/hormone-sensitive lipase pathways. One patient with toxicity was on ursodeoxycholic acid, possibly influencing bile acid-related metabolites. Overall, early urinary adverse events in VMAT were associated with lipid metabolism dysregulation. No metabolites remained significant after false discovery rate correction, and this exploratory, hypothesis-generating analysis suggested that urinary metabolomics may serve as a non-invasive biomarker platform for toxicity prediction, warranting validation in larger cohorts.

Correspondence to: Professor Satoru Monzen, Department of Radiation Science, Hirosaki University Graduate School of Health Sciences, 66-1 Hon-cho, Hirosaki, Aomori 036-8564, Japan
E-mail: monzens@hirosaki-u.ac.jp

Key words: urinary metabolite, radiotherapy, prostate cancer, adverse events

Introduction

Prostate cancer is the second most commonly diagnosed malignancy in men worldwide, with an estimated 1.5 million new cases and approximately 400,000 deaths annually (1). In Japan, diagnosis and treatment decisions are guided by prostate-specific antigen (PSA) levels, Gleason score, and the National Comprehensive Cancer Network (NCCN) risk classification (2).

Radiotherapy remains a key treatment option for localized prostate cancer. Volumetric Modulated Arc Therapy (VMAT), an advanced technique within intensity-modulated radiotherapy, delivers highly conformal dose distributions while minimizing exposure to surrounding normal tissues (3). Despite these advantages, early urinary toxicities-including frequency, dysuria, and reduced urinary flow-remain common. Even low-grade (Grade 1) toxicities can significantly affect quality of life. However, robust biomarkers capable of predicting such events are still lacking.

Radiation exposure not only causes direct and indirect DNA damage but also induces substantial alterations in proteins and lipids, leading to oxidative stress and inflammatory responses (4). These biological disturbances are reflected in shifts in metabolite profiles. Metabolomics, which comprehensively characterizes small molecules in biological samples, has therefore gained increasing attention in radiation research as a means to capture these downstream effects (5,6). Urinary metabolomics, in particular, offers a non-invasive method to monitor treatment-related physiological changes (7). In our previous analysis of this dataset, we examined the role of phospholipase A2 (PLA2) activity during VMAT and identified its potential as a predictor of acute urinary toxicity (8). Although this finding highlighted an important enzymatic pathway, it provided only a partial perspective on the broader

metabolic disruptions caused by irradiation. A narrow focus on PLA2 leaves open the question of whether other lipid-related pathways-such as triglyceride (TG) hydrolysis, bile acid (BA)-mediated mechanisms, or cholesterol ester turnover-also contribute to urinary adverse events.

A secondary analysis of the same comprehensive dataset provides an opportunity to overcome this limitation. By re-evaluating all 630 quantified metabolites with a focus on treatment-related toxicity rather than a single enzymatic pathway, we can uncover novel candidate biomarkers, delineate alternative metabolic routes, and reinforce the biological rationale for metabolomic monitoring in radiotherapy. In particular, correlation-based ranking and network analysis enable the detection of coordinated alterations across lipid classes, rather than isolated enzymatic signals. In the present study, we conducted a secondary analysis of a previously published urinary metabolomics dataset generated in an original clinical study during VMAT (8) and deposited in MetaboBank (accession numbers MTBKS242 and MTBKS243). No new patient recruitment or urine collection was performed for this secondary analysis.

Accordingly, the present study aimed to identify urinary metabolites and metabolic pathways associated with early urinary adverse events during VMAT, extending beyond PLA2 to achieve a more integrative understanding of lipid metabolism under irradiation.

Materials and methods

Study design. The present study is a secondary analysis of a previously published urinary metabolomics dataset originally generated in a clinical study during VMAT and made publicly available in MetaboBank (8). No new patient recruitment, intervention, sample collection, or metabolomic data generation was performed as part of the present study. As this study exclusively analyzed de-identified data obtained from a public repository, additional ethical approval was not required. The cohort comprised 11 males (0 females), with a median age of 70 years (range, 59-75), who underwent VMAT at Hirosaki University Hospital between June 2021 and March 2022, as described in the original report (8). All patients received 76 Gy in 38 fractions (2 Gy per fraction, five fractions weekly). Clinical characteristics-including age, PSA level, Gleason score, TNM stage, NCCN risk classification, prior or concurrent hormone therapy, and acute adverse events-were documented in the initial publication (8). Seven patients experienced Grade 1 urinary toxicities (frequency, dysuria, or decreased flow), while four patients reported no acute urinary events. Toxicities were graded according to the Common Terminology Criteria for Adverse Events, version 5.0 (9).

Metabolomics profiling. In the original clinical study (8), daily first-morning urine samples (10 ml) had been self-collected during the treatment period using a standardized collection device and stored at -80˚C until analysis, as previously described (8). Metabolomic profiling was performed with the MxP® Quant 500 kit (Biocrates Life Sciences AG, Innsbruck, Austria), enabling quantification of 630 metabolites, comprising 107 small molecules and 523 lipids. Sample preparation, LC-MS/MS acquisition, and quality control procedures followed the manufacturer's standard operating protocol and were fully detailed in the original report (8). Briefly, metabolite concentrations were determined using multiple reaction monitoring with isotope-labeled internal standards and normalized to urinary creatinine to correct for dilution variability. The complete metabolomics dataset is publicly available in MetaboBank under accession numbers MTBKS242 (https://mb2.ddbj.nig.ac.jp/study/MTBKS242.html) and MTBKS243 (https://mb2.ddbj.nig.ac.jp/study/MTBKS243.html), as described in the original report (8).

Statistical analysis. Because this study is exploratory and hypothesis-generating, statistical interpretation focused on the direction and magnitude of associations rather than confirmatory inference. For each patient and each metabolite, Spearman's rank correlation coefficient (ρ) was calculated between the number of delivered radiation fractions and the creatinine-normalized metabolite concentration. Patient-level ρ values were summarized within each group [AE(+) vs. AE(-)], and metabolites were ranked by the median ρ in each group. To screen for group-specific metabolic alterations, we used a bidirectional rank-based screening as follows: (i) the top 60 metabolites with the highest median ρ in AE(+) were compared with the bottom 60 metabolites with the lowest median ρ in AE(-); and (ii) the top 60 metabolites in AE(-) were compared with the bottom 60 metabolites in AE(+). Overlapping metabolites across these contrasted sets were carried forward for network analysis (a predefined exploratory threshold). Network analyses of the selected metabolites were performed using OmicsNet 2.0 (https://www.omicsnet.ca) (10), which integrates curated metabolite-enzyme and pathway interaction data from public databases including KEGG, HMDB, Reactome, and SMPDB. Networks were generated under the Homo sapiens setting using the platform's default metabolite-enzyme interaction resources. Statistical analyses were carried out with Statcel 5 (OMS Publishing Inc., Saitama, Japan). Between-group differences in patient-level ρ values were assessed using Mann-Whitney U tests. P-values were adjusted for multiple testing using the Benjamini-Hochberg false discovery rate (FDR) procedure; nominal p-values and FDR-adjusted q-values are reported. FDR adjustment was implemented in Python (Google Colab) using statsmodels.stats.multitest (method='fdr_bh'). In addition, changes in metabolite levels (Δ) were calculated for each patient as the difference between metabolite levels at the end of radiotherapy (fraction 38) and baseline (fraction 0). These Δ values were compared between the AE(+) and AE(-) groups using the Mann-Whitney U test. This analysis was performed as a complementary evaluation of pre-post changes.

Sensitivity analysis. To assess potential confounding by concomitant ursodeoxycholic acid (UDCA) treatment, we repeated the between-group comparison after excluding the single AE(+) patient receiving UDCA (Pt.7) and summarized the results for the key metabolites in Tables SI and SII.

Results

Patient characteristics. The clinical profiles of the 11 patients included in this secondary analysis are summarized in

Table I. Clinical characteristics of patients.

Patient no.	TNM classification	Stage (risk level)	Gleason score (prior to the start of irradiation)	Age, years	Delivered fractions	Urine samples, n	PSA, ng/ml	Hormone therapy	AE	CC
1	$cT_3N_0M_0$	III (high)	5+4	69	38	8	5.10	CAB (leuprorelin acetate + estramustine phosphate sodium hydrate); leuprorelin acetate SR	(+)	Urethral pressure, painful urination
2	$cT_{3a}N_0M_0$	III (high)	4+3	69	38	8	18.44	CAB; leuprorelin acetate SR	(+)	Urethritis, painful urination, difficulty urinating, frequent urination
3	$cT_{2b}N_0M_0$	II (mid)	5+4	72	38	8	26.60	CAB	(+)	Frequent urination
4	$cT_{3a}N_0M_0$	III (high)	5+3	61	38	8	23.30	CAB; bicalutamide for 8 weeks	(+)	Urethritis, difficulty urinating
5	$cT_3N_0M_0$	III (high)	4+5	75	38	7	4.05	NHT	(+)	Frequent urination, decreased urinary flow
6	$cT_{1c}N_0M_0$	II (mid)	3+4	71	38	7	8.80	Bicalutamide	(+)	Frequent urination
7	$cT_{2b}N_0M_0$	II (mid)	4+3	71	38	7	4.44	CAB using bicalutamide and leuprorelin acetate SR, and ursodeoxy cholic acid	(+)	Frequent urination, decreased urinary flow
8	$cT_{2b}N_0M_0$	II (mid)	3+4	68	38	5	7.23	CAB	(-)	-
9	$cT_{2a}N_0M_0$	II (high)	4+4	73	38	5	4.38	Degarelix acetate + estramustine phosphate sodium hydrate	(-)	-
10	$cT_{1c}N_0M_0$	I (mid)	3+3	70	38	5	27.20	CAB; leuprorelin acetate SR	(-)	-
11	$cT_{1c}N_0M_0$	I (low)	3+3	59	38	5	6.97	-	(-)	-

The age at the start of irradiation, baseline PSA level and Gleason score (assessed prior to the start of irradiation) are shown. AE(+) patients developed Grade 1 urinary toxicities during volumetric modulated arc therapy, including increased urinary frequency, dysuria or decreased urinary flow, according to Common Terminology Criteria for Adverse Events version 5.0. CAB, combined androgen blockade; NHT, neoadjuvant hormonal therapy; AE, adverse event; CC, chief complaint; PSA, prostate-specific antigen; SR, sustained release.

Table I. The median age was 70 years (range, 59-75). Median PSA level was 7.23 ng/ml, and the median Gleason score was 7. According to the NCCN risk classification, 6 patients (54.5%) were categorized as high risk. Seven patients (63.6%)

Table II. Median (range) patient-level Spearman's rank correlation coefficients (ρ) between radiation fraction number and metabolite concentration in the AE(+) and AE(-) groups for metabolites showing opposite directional correlations.

	Metabolites			
AE group	CE (20:4)	TDCA	TG (18:0_32:2)	TG (18:3_34:1)
AE(+)	0.34 (0.10 to 0.67)	0.22 (-0.20 to 0.70)	0.22 (-0.16 to 0.46)	0.21 (-0.16 to 0.46)
AE(-)	-0.35 (-0.80 to 0.30)	-0.37 (-0.78 to -0.30)	-0.46 (-0.90 to 0.05)	-0.60 (-0.90 to -0.40)

Statistical comparisons of patient-level ρ values between groups were performed using the Mann-Whitney U test with Benjamini-Hochberg false discovery rate correction. Full statistical results are provided in Table SII. AE, adverse event; CE, cholesteryl ester; TDCA, taurodeoxycholic acid; TG, triglyceride.

developed Grade 1 urinary adverse events [AE(+)], while 4 patients (36.4%) experienced no acute urinary events [AE(-)].

Correlation analysis of urinary metabolites. In total, 630 urinary metabolites quantified by the MxP® Quant 500 kit were analyzed. For each patient, Spearman's rank correlation coefficients (ρ) were calculated between the number of delivered radiation fractions and the creatinine-normalized concentrations of each metabolite, yielding a patient-level ρ for each metabolite. Between-group differences in patient-level ρ values were then assessed using Mann-Whitney U tests, and p-values were adjusted using Benjamini-Hochberg FDR correction. After FDR correction across 630 metabolites, none of the metabolites remained significant (minimum q-value=0.49) (Table SII). Therefore, the metabolites highlighted below should be interpreted as exploratory candidates based on consistent directional differences and nominal associations. We focused on metabolites that demonstrated strong positive or negative correlations with radiation fraction number based on rank order of patient-level Spearman's ρ values. Specifically, because the sample size was limited and the analysis involved a large number of metabolites (n=630), strict multiple-testing correction markedly reduced statistical power. Therefore, to identify biologically meaningful directional patterns while limiting the number of candidates for downstream network analysis, a rank-based screening strategy focusing on metabolites showing the strongest positive or negative correlations with radiation fraction number was adopted. Specifically, this approach aimed to identify metabolites showing opposite directional trends between groups [those increasing with treatment in the AE(+) group while decreasing in the AE(-) group, and vice versa]. Specifically, the top 60 metabolites showing the strongest positive correlations with fraction number in AE(+) patients and the 60 metabolites showing the strongest negative correlations (lowest ρ values) in AE(-) patients were selected. Thus, the 'top 60' refers to metabolites with the most extreme correlation coefficients in each direction based on rank order, including those with the strongest negative correlations. Conversely, metabolites with the opposite directional patterns [top 60 metabolites with the strongest positive correlations in AE(-) patients and top 60 metabolites with the strongest negative correlations in AE(+) patients] were also examined. This bidirectional screening approach was designed to identify metabolites exhibiting consistent but opposite directional changes between the AE(+) and AE(-) groups. The overlap structure of these ranked sets is summarized in Fig. 1, and this bidirectional screening yielded 9 overlapping metabolites (Tables II and III). Of these, 4 metabolites-cholesteryl ester [CE(20:4)], taurodeoxycholic acid (TDCA), TG(18:0_32:2), and TG(18:3_34:1)-showed positive correlation in AE(+) but negative correlation in AE(-). Conversely, 5 metabolites-phosphatidylcholine (PC aa C42:2), PC ae C42:1, TG(16:0_38:1), fatty acid [FA(20:2)], and diglyceride [DG(18:1_18:1)]-demonstrated the opposite trend (positive in AE(-), negative in AE(+)). As a complementary analysis, changes in metabolite levels (Δ) between baseline (fraction 0) and the end of radiotherapy (fraction 38) were compared between AE(+) and AE(-) groups. The results of this Δ-based comparison are summarized in Table SI. Overall, several metabolites exhibited opposite directional changes between groups, consistent with the correlation-based findings. Among these, TG (16:0_38:1) and DG (18:1_18:1) showed nominally significant differences between groups in the primary analysis, although this was not consistently observed in the sensitivity analysis. These results should be interpreted as exploratory.

Network analysis of lipid metabolism. To explore the biological significance of the overlapping metabolites, interaction networks were generated using OmicsNet 2.0. Metabolites that increased in AE(+) patients were enriched in pathways involving cholesterol esters, BAs, and TGs (Fig. 2). In contrast, those that decreased in AE(+) were predominantly linked to diglycerides, fatty acids, and PCs (Fig. 3). Expanded network analysis further identified 29 metabolites connecting PCs with FAs (Fig. 4; Table SIII) and 12 metabolites bridging fatty acids with diglycerides/TGs (Fig. 5; Table SIV). These coordinated alterations pointed to a disruption in lipolytic processes. Sensitivity analysis excluding the UDCA-treated patient (Pt.7) showed that the nominal associations and directional patterns for the key metabolites were largely preserved (Table SII).

In particular, TDCA remained nominally different between groups (p=0.01), although q-values increased after exclusion due to reduced sample size.

Hypothesized involvement of TG hydrolysis. Building on these results, we focused on the lipolysis pathway, which converts TGs into fatty acids and glycerides. A schematic representation is shown in Fig. 6 (Table SV). The simultaneous increase in specific TG isomers and paradoxical reduction in their corresponding fatty acids suggested a potential inhibition of lipolysis. In addition, alterations

Table III. Median (range) patient-level Spearman's rank correlation coefficients (ρ) between radiation fraction number and metabolite concentration in the AE(-) and AE(+) groups for metabolites showing opposite directional correlations.

	Metabolites				
AE group	PC aa C42:2	TG (16:0_38:1)	PC ae C42:1	FA (20:2)	DG (18:1_18:1)
AE(-)	0.61 (0.53 to 0.90)	0.48 (0.20 to 0.67)	0.36 (0.20 to 0.80)	0.35 (-0.20 to 0.60)	0.32 (-0.90 to 0.90)
AE(+)	-0.19 (-0.77 to 0.06)	-0.23 (-0.57 to 0.05)	-0.15 (-0.45 to 0.29)	-0.22 (-0.76 to 0.36)	-0.35 (-0.76 to -0.02)

Statistical comparisons of patient-level ρ values between groups were performed using the Mann-Whitney U test with Benjamini-Hochberg false discovery rate correction. Full statistical results are provided in Table SII. AE, adverse event; DG, diglyceride; FA, fatty acid; PC, phosphatidylcholine; TG, triglyceride.

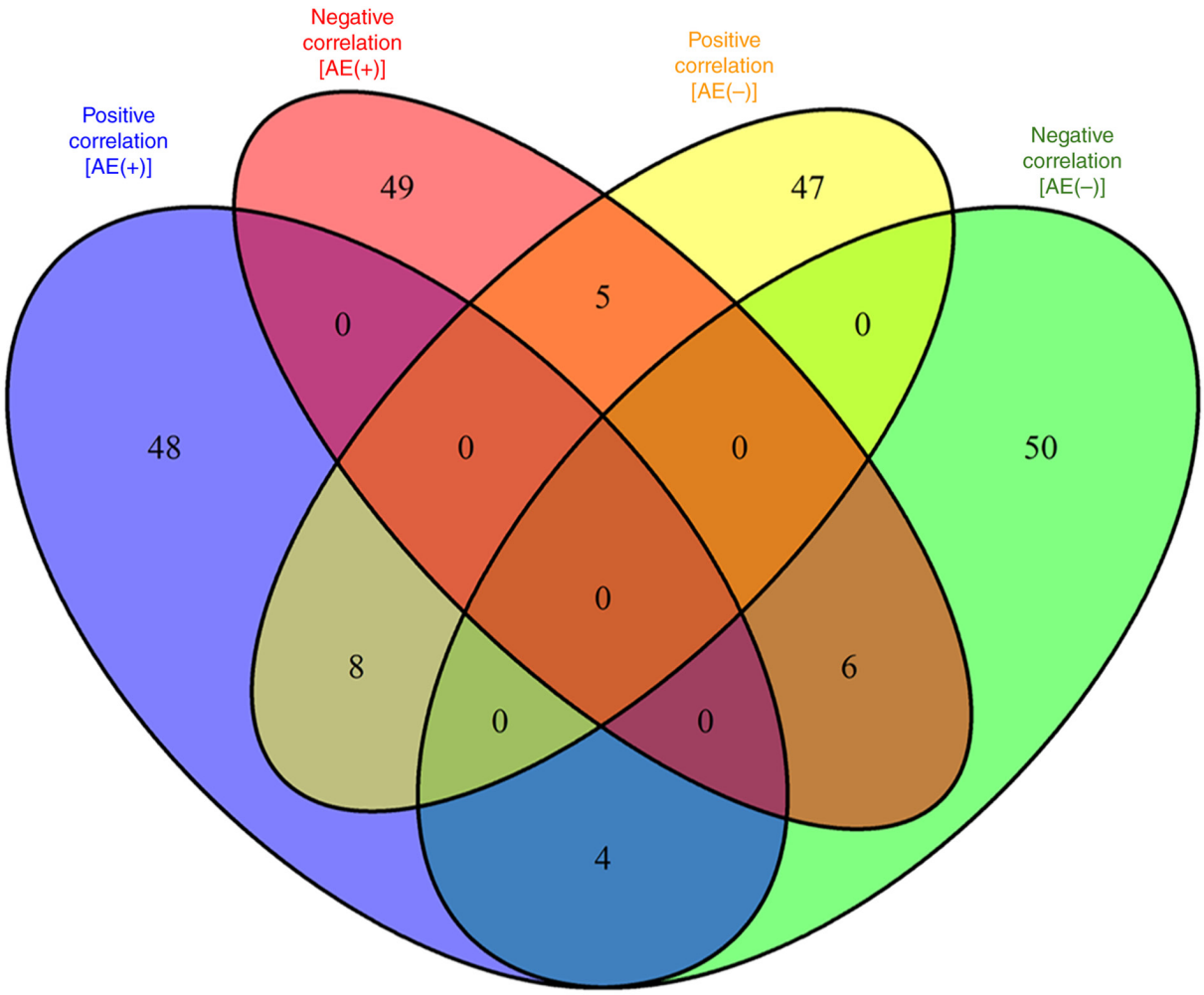

Figure 1. Venn diagram of rank-based metabolite sets derived from patient-level Spearman's rank correlation coefficients (ρ). Metabolites were ranked according to the median ρ between radiation fraction number and metabolite concentration within each group. Four ranked sets were defined: Positive correlation [AE(+)], positive correlation [AE(-)], negative correlation [AE(-)] and negative correlation [AE(+)]. Overlaps among these sets with opposing correlation directions between the AE(+) and AE(-) groups were examined to identify metabolites showing opposite directional correlation patterns. AE, adverse event; negative correlation [AE(-)], top 60 negatively correlated metabolites in the AE(-) group; negative correlation [AE(+)], top 60 negatively correlated metabolites in the AE(+) group; positive correlation [AE(-)], top 60 positively correlated metabolites in the AE(-) group; positive correlation [AE(+)], top 60 positively correlated metabolites in the AE(+) group.

in cholesteryl ester metabolism appeared to be involved. Collectively, these exploratory findings suggest that early urinary adverse events during VMAT may be linked to dysregulated lipid metabolism, particularly impaired hydrolysis of TGs into fatty acids.

Discussion

In this secondary analysis of urinary metabolomics from patients receiving VMAT for localized prostate cancer, we observed distinct lipid metabolic alterations showing

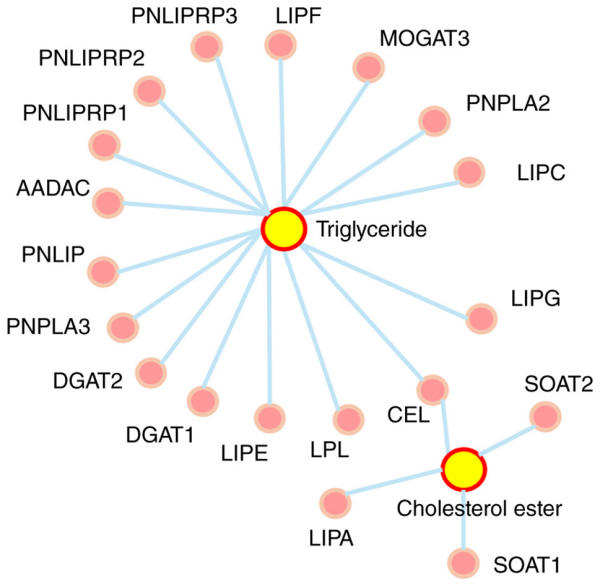

Figure 2. Network of metabolites positively correlated in the AE(+) group and negatively correlated in the AE(-) group. The network centers on triglyceride and cholesterol ester nodes connected to enzymes or proteins involved in lipid hydrolysis. AE, adverse event.

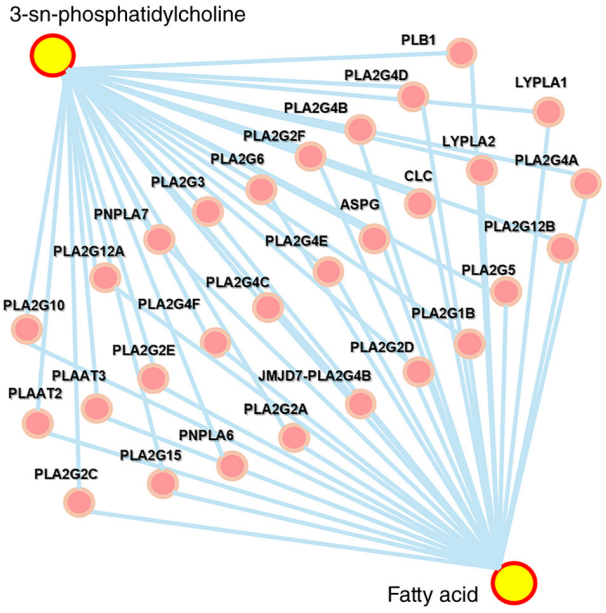

Figure 4. Enlarged subnetwork centered on 3-sn-phosphatidylcholine and fatty acid. The red nodes represent 29 enzymes and interacting molecules connecting these metabolites in the network analysis.

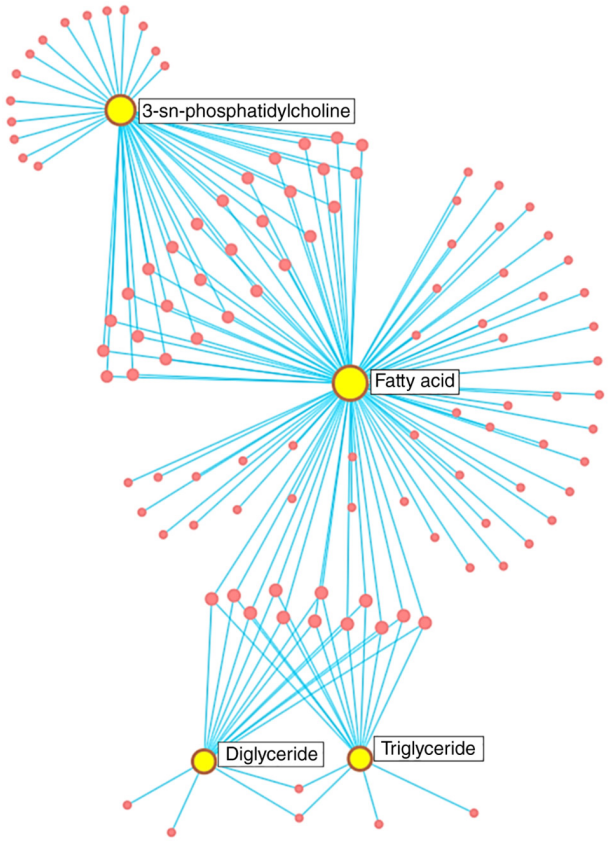

Figure 3. Network of metabolites positively correlated in the AE(-) group and negatively correlated in the AE(+) group. Yellow nodes represent key lipid classes (fatty acid, triglyceride, diglyceride and 3-sn-phosphatidylcholine), and red nodes represent associated enzymes and interacting molecules derived from curated pathway databases. AE, adverse event.

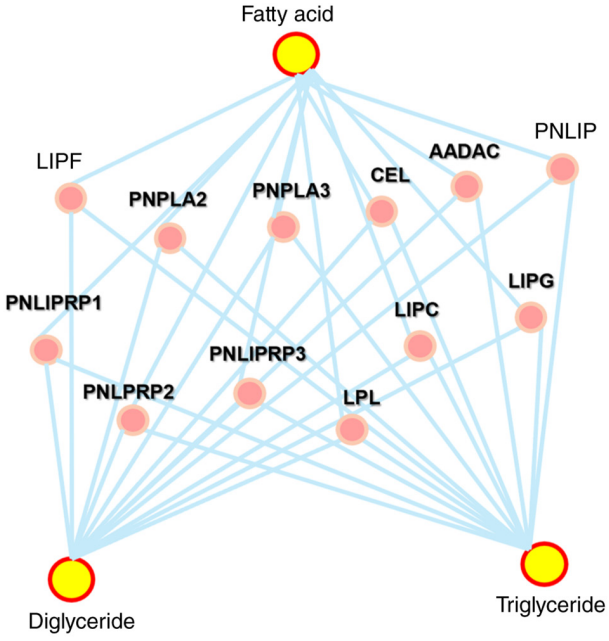

Figure 5. Interaction network centered on fatty acid, diglyceride and triglyceride. A total of 12 associated enzymes and interacting proteins linking these lipid classes are shown as red nodes.

directional differences between AE(+) and AE(-) groups; however, none of the metabolites remained statistically significant after FDR correction. Four metabolites-CE(20:4), TDCA, TG(18:0_32:2), and TG(18:3_34:1)-showed positive correlations with radiation fractions in AE(+) but negative correlations in AE(-), whereas five metabolites-PC aa C42:2, PC ae C42:1, TG(16:0_38:1), FA(20:2), and DG(18:1_18:1)-displayed the opposite pattern. Network analysis revealed convergence on lipid pathways, particularly TG hydrolysis into fatty acids.

We previously reported phospholipase A2 (PLA2) activity in urinary metabolites as a potential biomarker for predicting acute toxicities during VMAT (8). While that work

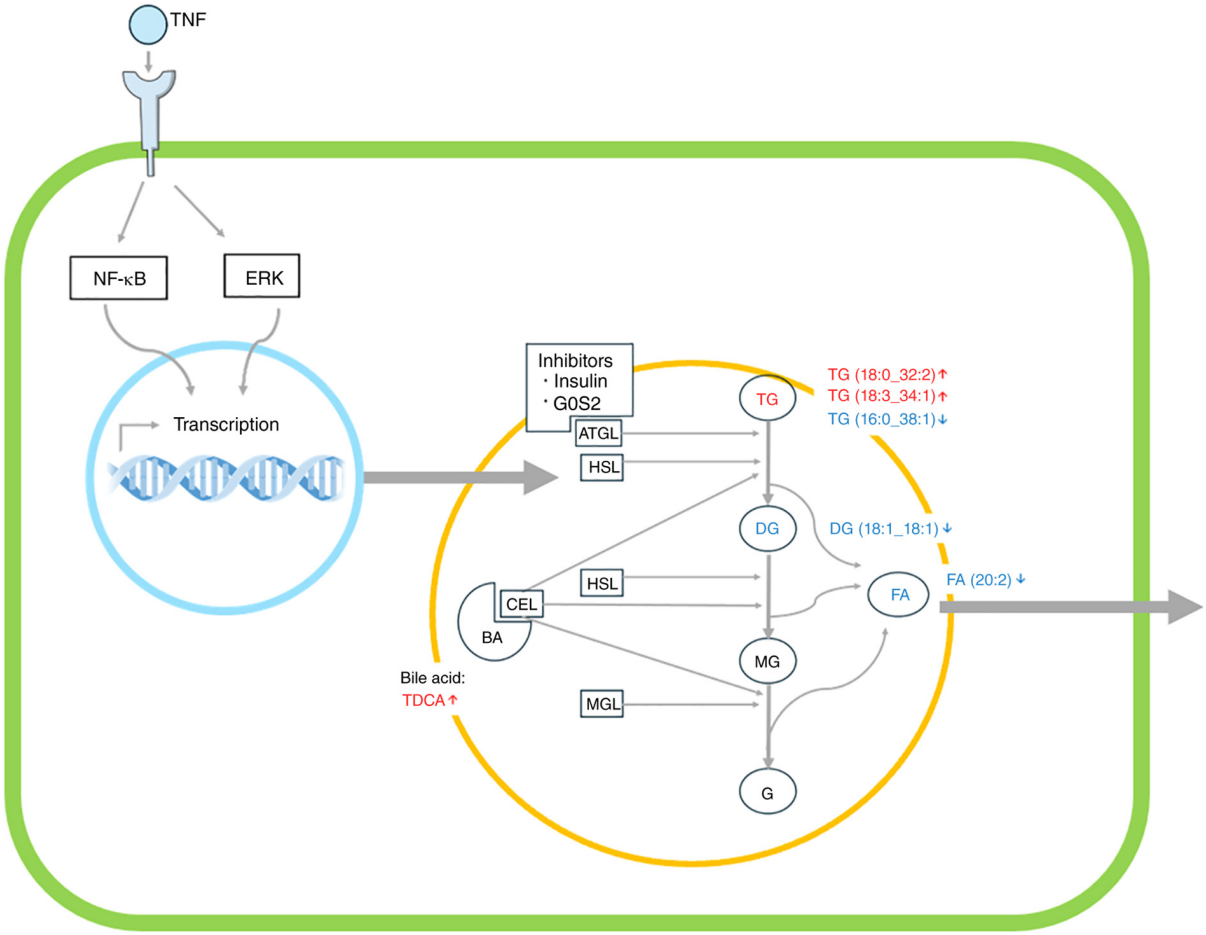

Figure 6. Schematic of TG hydrolysis (lipolysis) and associated intermediates. TNF signaling via NF-κB and ERK may influence transcriptional regulation of lipolytic enzymes. Inhibitors, including insulin and G0S2, suppress ATGL activity. Observed metabolite changes in the adverse event-positive group are indicated by arrows. ATGL, adipose triglyceride lipase; HSL, hormone-sensitive lipase; MGL, monoglyceride lipase; CEL, carboxyl ester lipase; TG, triglyceride; DG, diglyceride; MG, monoglyceride; FA, fatty acid; BA, bile acid; TDCA, taurodeoxycholic acid; G, glycerol.

emphasized phospholipid remodeling, the present analysis broadens the perspective to the lipid network as a whole. The discordant behavior of TGs and their corresponding fatty acids points to impaired lipolysis as a candidate mechanism for urinary AEs, thereby complementing earlier findings by shifting from a single enzymatic activity to a pathway-level view.

Lipolysis proceeds through sequential hydrolysis of TGs by adipose TG lipase (ATGL), hormone-sensitive lipase (HSL), and monoglyceride lipase, ultimately producing free fatty acids and glycerol (11). Cholesteryl ester lipase also contributes by hydrolyzing cholesterol esters and TGs (12). The paradoxical accumulation of certain TG species with reduced levels of corresponding fatty acids in AE(+) patients suggests suppression of this pathway. Possible inhibitory mechanisms include G0/G1 switch gene 2 (G0S2), a direct ATGL inhibitor (11), and insulin-mediated downregulation of HSL via cAMP signaling (12). Furthermore, cytokines such as TNF-α are known to influence lipolysis through NF-κB and ERK pathways, potentially intersecting with radiation-induced inflammation (13). Collectively, these findings are consistent with the possibility that radiation perturbs lipolytic regulation, leading to TG accumulation, reduced fatty acid release, which may be associated with urinary toxicity.

Only limited urinary biomarkers have been investigated for predicting early urinary AEs during radiotherapy. Previous studies have primarily focused on inflammatory cytokines (e.g., IL-6, IL-8), oxidative stress markers such as 8-hydroxy-2'-deoxyguanosine (8-OHdG), or tubular injury markers including NGAL and β2-microglobulin. These markers reflect downstream inflammation or tissue injury but do not capture broader metabolic pathway alterations. To our knowledge, comprehensive urinary metabolomic profiling integrated with fraction-dependent correlation analysis has not previously been applied to early urinary toxicity during VMAT. Our pathway-oriented, lipid-focused analysis therefore provides a systems-level perspective that extends beyond single-marker approaches. The identification of lipid metabolic dysregulation highlights the potential of urinary metabolomics for toxicity monitoring. The involvement of bile acid-related metabolites such as TDCA further underscores the need to consider background medications when interpreting metabolomic findings.

This study has several limitations. First, the sample size was small (n=11), which precludes statistical generalization and limits power. Second, only Grade 1 urinary toxicities were observed, leaving it unclear whether similar metabolic alterations would be observed in higher-grade AEs. Third,

as a secondary analysis of an existing dataset, this work is hypothesis-generating rather than causal. In addition, none of the identified metabolites remained statistically significant after FDR correction, underscoring the exploratory nature of these findings. Although Grade 1 urinary AEs are clinically mild, we consider them to reflect early radiation-induced biological perturbations in the urinary tract that may precede more severe toxicity. Whether similar or amplified metabolic patterns are observed in Grade ≥2 urinary AEs should be evaluated in larger prospective cohorts. One AE(+) patient received ursodeoxycholic acid (UDCA), which could theoretically influence BA-related metabolites. However, a sensitivity analysis excluding this patient yielded similar nominal associations and preserved the directional patterns of the key metabolites (Table SI and SII), suggesting that our main interpretation was unlikely to be entirely driven by this single case.

Future research should validate these findings in larger, prospectively collected cohorts with broader toxicity profiles. Complementary experimental approaches, such as in vitro irradiation models or enzymatic assays, may help clarify whether the paradoxical increase in TGs alongside reduced fatty acids reflects inhibition of lipolysis. Such studies would provide mechanistic evidence for the associations reported here and enhance the translational potential of urinary metabolomics in radiotherapy.

In summary, this study suggests that early urinary AEs during VMAT may be associated with dysregulated lipid metabolism, particularly impaired hydrolysis of TGs into fatty acids. These results build upon our prior findings on PLA2 activity (8) and support the potential of urinary metabolomics as a non-invasive biomarker platform for predicting radiotherapy-related toxicities. Although exploratory, this analysis generates testable hypotheses that warrant validation in larger cohorts and mechanistic studies to better define the role of lipid metabolism in radiation-induced urinary toxicity.

Acknowledgements

Not applicable.

Funding

The present study was supported by the Japan Society for the Promotion of Science, Grants-in-Aid for Scientific Research (B) (grant no. 23K21419) and Grant-in-Aid for Challenging Research (grant no. 25K22722).

Availability of data and materials

The data generated in the present study are included in the figures and/or tables of this article.

Authors' contributions

MF and SM designed the study, prepared the manuscript draft and substantively participated in the manuscript revision. MF, YT, HO and SM analyzed all biological data. SM supervised the study, critically reviewed the manuscript, and provided final approval of the version to be submitted and published. MF, YT, HO and SM confirm the authenticity of all the raw data. All authors have read and approved the final version of the manuscript.

Ethics approval and consent to participate

Not applicable.

Patient consent for publication

Not applicable.

Competing interests

The authors declare that they have no competing interests.

References

1. Bray F, Laversanne M, Sung H, Ferlay J, Siegel RL, Soerjomataram I and Jemal A: GLOBOCAN estimates of incidence and mortality worldwide for 36 cancers in 185 countries. CA Cancer J Clin 74: 229-263, 2024.
2. Kohjimoto Y, Uemura H, Yoshida M, Hinotsu S, Takahashi S, Takeuchi T, Suzuki K, Shinmoto H, Tamada T, Inoue T, *et al*: Japanese clinical practice guidelines for prostate cancer 2023. Int J of Urol 31: 1180-1221, 2024.
3. Japanese Society for Radiation Oncology (ed): JASTRO Guidelines 2024 for Radiotherapy Treatment Planning. 6th edition. Kanehara & Co., Ltd., Tokyo, 2024 (In Japanese). https://www.kanehara-shuppan.co.jp/books/detail.html?isbn=9784307071314
4. Kim JH, Jenrow KA and Brown SL: Mechanisms of radiation-induced normal tissue toxicity and implications for future clinical trials. Radiat Oncol J 32: 103-115, 2014.
5. Johnson CH, Patterson AD, Krausz KW, Lanz C, Kang DW, Luecke H, Gonzalez FJ and Idle JR: Radiation metabolomics. 4. UPLC-ESI-QTOFMS-Based metabolomics for urinary biomarker discovery in gamma-irradiated rats. Radiat Res 175: 473-484, 2011.
6. Goudarzi M, Weber WM, Mak TD, Chung J, Doyle-Eisele M, Melo DR, Brenner DJ, Guilmette RA and Fornace AJ Jr: Metabolomic and lipidomic analysis of serum from mice exposed to an internal emitter, cesium-137, using a shotgun LC-MS(E) approach. J Proteome Res 14: 374-384, 2015.
7. Chen CL, Chen YT, Liao WY, Chang YS, Yu JS and Juo BR: Urinary metabolomic analysis of prostate cancer by UPLC-FTMS and UPLC-Ion Trap MSn. Diagnostics (Basel) 13: 2270, 2023.
8. Obara H, Tatara Y, Monzen S, Murakami S, Yamamoto H, Kimura N, Suzuki M, Komai F, Narita M, Hatayama Y and Aoki M: Exploring predictive molecules of acute adverse events in response to volumetric-modulated arc therapy for prostate cancer using urinary metabolites. Mol Clin Oncol 21: 62, 2024.
9. National Cancer Institute: Common Terminology Criteria for Adverse Events (CTCAE), Version 5.0. Bethesda, MD: U.S. Department of Health and Human Services, National Institutes of Health, 2017. https://dctd.cancer.gov/research/ctep-trials/for-sites/adverse-events/ctcae-v5-5x7.pdf
10. Zhou G and Xia J: OmicsNet: A web-based tool for creation and visual analysis of biological networks in 3D space. Nucleic Acids Res 46: W514-W522, 2018.
11. Lass A, Zimmermann R, Haemmerle G, Riederer M, Schoiswohl G, Schweiger M, Kienesberger P, Strauss JG, Gorkiewicz G and Zechner R: Adipose triglyceride lipase-mediated lipolysis of cellular fat stores is activated by CGI-58 and defective in Chanarin-Dorfman Syndrome. Cell Metab 3: 309-319, 2006.
12. Hui DY and Howles PN: Carboxyl ester lipase: Structure-function relationship and physiological role in lipoprotein metabolism and atherosclerosis. J Lipid Res 43: 2017-2030, 2002.
13. Grant RW and Stephens JM: Fat in flames: Influence of cytokines and pattern recognition receptors on adipocyte lipolysis. Am J Physiol Endocrinol Metab 309: E205-E213, 2015.